Ion-beam–plasma interaction effects on electrostatic solitary wave propagation in ultradense relativistic quantum plasmas

I. S. Elkamash,[1,2,*] I. Kourakis,[1,†] and F. Haas[3,‡]

[1]*Centre for Plasma Physics, Queen's University Belfast, Belfast BT7 1NN, Northern Ireland, United Kingdom*
[2]*Physics Department, Faculty of Science, Mansoura University, 35516 Mansoura, Egypt*
[3]*Instituto de Física, Universidade Federal do Rio Grande do Sul, Avenida Bento Gonçalves 9500,*
CEP 91501-970 Porto Alegre, Rio Grande do Sul, Brazil

Understanding the transport properties of charged particle beams is important not only from a fundamental point of view but also due to its relevance in a variety of applications. A theoretical model is established in this article, to model the interaction of a tenuous positively charged ion beam with an ultradense quantum electron-ion plasma, by employing a rigorous relativistic quantum-hydrodynamic (fluid plasma) electrostatic model proposed in McKerr *et al.* [M. McKerr, F. Haas, and I. Kourakis, Phys. Rev. E **90**, 033112 (2014)]. A nonlinear analysis is carried out to elucidate the propagation characteristics and the existence conditions of large amplitude electrostatic solitary waves propagating in the plasma in the presence of the beam. Anticipating stationary profile excitations, a pseudomechanical energy balance formalism is adopted to reduce the fluid evolution equation to an ordinary differential equation. Exact solutions are thus obtained numerically, predicting localized excitations (pulses) for all of the plasma state variables, in response to an electrostatic potential disturbance. An ambipolar electric field form is also obtained. Thorough analysis of the reality conditions for all variables is undertaken in order to determine the range of allowed values for the solitonic pulse speed and how it varies as a function of the beam characteristics (beam velocity and density).

I. INTRODUCTION

Quantum plasmas are ubiquitous in astrophysical environments, e.g., in planetary interiors and in white dwarfs, magnetars, and pulsars [1,2], and are also relevant in applications, e.g., related to quantum wells [3], plasmonics [4], spintronics [5], and ultracold plasmas [6]. Quantum plasma effects are also of relevance in solids, in particular metals, for which the conduction electrons can be viewed as a mobile plasma neutralized by background ions [7]. Quantum degeneracy effects start playing a significant role when the *de Broglie* length λ_B, which represents the spatial extension of the particle's wave function, is larger than the average interparticle distance. Thus, the particle cannot be considered as pointlike any more, as in classical plasma, and quantum interference of overlapping particles' wave functions needs to be taken into account [8]. When the Fermi temperature exceeds the thermal temperature, the equilibrium distribution function changes from Maxwell-Boltzmann to a Fermi-Dirac distribution [9,10]. Quantum effects are manifested in dense plasma in various ways, e.g., quantum statistical pressure may be dominant (exceeding the thermal pressure) and quantum wave diffraction or tunneling (modeled via a Bohm potential) and adopting a quantum exchange and correlation potential (due to spin effects) may be necessary in the modeling [11–13].

Ion beams are relevant in various real applications of plasmas, including heavy-ion inertial fusion [14–16], intense laser-produced proton beams for laser-based fast ignition (inertial confinement fusion) schemes [17–20], semiconductor lasers [21–23], and electron cooling of ion beams [24,25]. Nonlinear electrostatic localized modes (nonlinear waves) occur widely in plasmas [26,27]; the impact of ion beam injection in a plasma has been studied theoretically [28] and also numerically, e.g., via particle-in-cell (PIC) simulations [29–33].

Relativistic effects become relevant either when the bulk (fluid) velocity of a plasma fluid component is comparable in order of magnitude to the velocity of light or when the average kinetic energy of the charged particles is greater than the electron rest energy (e.g., the Fermi energy of plasma $E_{Fe} \geqslant mc^2$) [34]. This may happen under the influence of an ultrastrong electromagnetic field, e.g., a laser beam [35,36]. In the framework of interaction of intense laser pulses with underdense plasma, relativistic localized solitary pulses, commonly regarded as self-trapped localized structures, have been detected experimentally [37–39] and have also been modeled numerically, via PIC simulations [40,41]. A wide variety of nonlinear mechanisms may affect the formation and propagation of relativistic solitons, such as finite particle inertia, relativistic particle mass variation, ponderomotive forces, etc. [42–44].

A comprehensive model was elaborated in Ref. [45], within the electrostatic approximation, taking into account (quantum) electron degeneracy in combination with a relativistic formulation of fluid dynamics. Subsequent work based on that model has revealed the existence of an acoustic and a Langmuir-like mode(s) [46], in analogy to the classical version of the problem [47], whose characteristics take into account relativistic and quantum effects (becoming important at high densities), as expected. When a tenuous ion beam penetrates the plasma [48], a second low-frequency acoustic mode arises; the energy excess due to the beam may then destabilize both acoustic modes, and a beam-plasma instability occurs [48].

*elkamashi@gmail.com

†IoannisKourakisSci@gmail.com; www.kourakis.eu

‡fernando.haas@ufrgs.br; www.professor.ufrgs.br/fernando-haas

For a tenuous beam, the instability growth rate is weak and fails to destabilize electrostatic vibrations, as it operates in a narrow wave number window.

In this article, we investigate, from first principles, the dynamical characteristics of localized modes (solitary waves) propagating in an ultradense electron-ion plasma permeated by a secondary ion beam. Building upon the formalism introduced in Ref. [45], here extended to accommodate the dynamics of the ion beam, a multifluid relativistic model for electrostatic plasma excitations is laid out in the next section and its validity and physical limitations are discussed. Nonlinear analysis based on a (Sagdeev type [49,50]) pseudopotential method is carried out in Sec. III, leading to a set of explicit expressions for the state variables in terms of the electrostatic potential (disturbance). The existence of localized forms (pulses) is possible in certain regions in parameter space, which are explored in Sec. IV. A parametric analysis follows, in Sec. V, elucidating the dependence of electrostatic pulse characteristics on the beam properties and other intrinsic plasma parameters. Our findings are finally summarized in Sec. VI.

II. A MULTIFLUID RELATIVISTIC PLASMA MODEL

We consider a three-component plasma consisting of a dominant ion population (mass m_i, positive charge $q_i = +Z_i e$), a secondary ion species, representing a tenuous beam (mass m_b, charge $q_b = +Z_b e$), and electrons (mass m_e, charge $-e$); e denotes the elementary (absolute) charge, as usual. We consider the spatial variation of the plasma (including the ion beam) to be in the longitudinal direction, so the plasma dynamics can be described by a one-dimensional (1D) geometry for simplicity. Our study relies on a multifluid approach introduced in the following paragraph. We assume from the outset that magnetic field generation may be neglected, within the electrostatic approximation, implying that the total current is negligible (nearly quiescent plasma); clearly, a very weak beam current is implied by this model, as the electrostatic approximation breaks down for strongly relativistic beam flows. Our description follows closely the electrostatic relativistic model proposed in Refs. [45,46], thus extending the analytical framework proposed therein to take into account the ion beam.

The dominant (positive) ion population will be treated as a cold (classical) fluid, for simplicity, a plausible assumption, given their high mass (compared to the electrons). The continuity and momentum equations of motion for the ion fluid respectively read

$$\frac{\partial(\gamma_i n_i)}{\partial t} + \frac{\partial}{\partial x}(\gamma_i n_i u_i) = 0, \tag{1}$$

$$\frac{\partial(\gamma_i u_i)}{\partial t} + u_i \frac{\partial(\gamma_i u_i)}{\partial x} = -\frac{eZ_i}{m_i}\frac{\partial\phi}{\partial x}, \tag{2}$$

where e is the electron charge, Z_i is the ion charge state, m_i is the ion mass, n_i is the ion fluid density, and u_i is the ion fluid speed. One recognizes the electrostatic force $q_i E$ in the right-hand side (RHS) of the momentum equation, where $E = -\partial\phi/\partial x$ is the electric field deriving from an electrostatic potential function ϕ.

The electron fluid equations read [45]

$$\frac{\partial(\gamma_e n_e)}{\partial t} + \frac{\partial}{\partial x}(\gamma_e n_e u_e) = 0, \tag{3}$$

$$\sqrt{1+\xi^2}\left[\frac{\partial(\gamma_e u_e)}{\partial t} + u_e \frac{\partial(\gamma_e n_e)}{\partial x}\right]$$
$$= \frac{e}{m_e}\frac{\partial\phi}{\partial x} - \frac{\gamma_e}{n_e m_e}\left(\frac{\partial P_e}{\partial x} + \frac{u_e}{c^2}\frac{\partial P_e}{\partial t}\right), \tag{4}$$

where m_e is the rest mass of the electron, n_e is the electron fluid (number) density, and u_e is the electron fluid speed. In the latter equation, the parameter $\xi = p_{Fe}/m_e c = hn_e/(4m_e c)$ is related to the (high) electron density (note that the classical limit is recovered for $h \to 0$).

In ultrahigh density conditions, electron degeneracy effects become significant and in fact far exceed the thermal pressure and, in very high densities, quantum pressure (expressed via a Bohm term [10]) too. The electrons then obey a Fermi-Dirac distribution, associated with an appropriate equation of state, which is incorporated in the model via the effective degeneracy pressure term in the highly relativistic limit, i.e., the last term in Eq. (4). Within our model, the quantum relativistic pressure term derives from the (1D) equation of state [45,51]:

$$P_e = \frac{2m_e^2 c^3}{h}[\xi(1+\xi^2)^{1/2} - \sinh^{-1}\xi]. \tag{5}$$

One also distinguishes in the RHS of Eq. (4) the electrostatic force term, which relates the momentum equation to the electrostatic potential ϕ.

The equations of motion for the ion beam read as follows:

$$\frac{\partial(\gamma_b n_b)}{\partial t} + \frac{\partial}{\partial x}(\gamma_b n_b u_b) = 0, \tag{6}$$

$$\frac{\partial(\gamma_b u_b)}{\partial t} + u_b \frac{\partial(\gamma_b u_b)}{\partial x} = -\frac{eZ_b}{m_b}\frac{\partial\phi}{\partial x}, \tag{7}$$

where m_b is the beam-ion mass, n_b is the beam-ion fluid density, and u_b is the beam-ion fluid speed. The relativistic factor $\gamma_j = 1/\sqrt{1 - u_j^2/c^2}$ (for $j = i,e,b$) appears in the fluid-dynamical equations, as a result of Lorentz transformations and resulting relations among different state variables between inertial frames.

The system is closed by Poisson's equation:

$$\frac{\partial^2\phi}{\partial x^2} = \frac{e}{\epsilon_0}(\gamma_e n_e - \gamma_i Z_i n_i - \gamma_b Z_b n_b). \tag{8}$$

In the above relations, c is the speed of light *in vacuo*, h is Planck's constant, ϵ_0 is the permittivity of free space, and e is the fundamental unit of electric charge. The quasineutrality condition, assumed to hold at equilibrium (only), can be written as follows: $n_{e0} - Z_i n_{i0} - Z_b \gamma_{b0} n_{b0} = 0$, where n_{e0}, n_{i0}, and n_{b0} are the unperturbed densities of the electron, ion, and beam-ion populations, respectively.

A. Rescaled (dimensionless) fluid-dynamical model

The fluid model can be cast in a dimensionless form, by adopting a set of characteristic scales:

$$t \rightarrow \omega_p t, \qquad x \rightarrow \omega_p x/c_s,$$

$$n_j \rightarrow n_j/n_{j0}, \qquad u_j \rightarrow u_j/c_s,$$

$$\text{and} \qquad \phi \rightarrow e\phi/2E_{\mathrm{Fe}}, \tag{9}$$

for $j = i,e,b$, where $\omega_p = \sqrt{Z_i e^2 n_{e0}/\epsilon_0 m_i}$ is the plasma frequency (in a beam-free electron-ion plasma). Note that the potential scale $(2E_{\mathrm{Fe}}/\phi)$ and the characteristic speed scale $c_s = \sqrt{2Z_i E_{\mathrm{Fe}}/m_i}$ are determined as functions of the
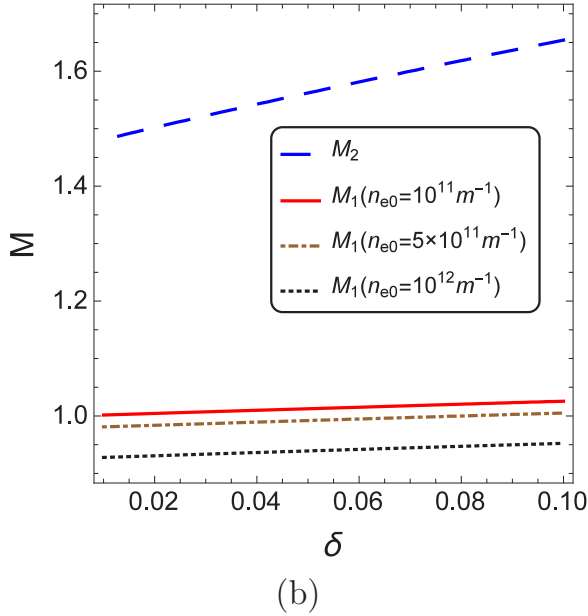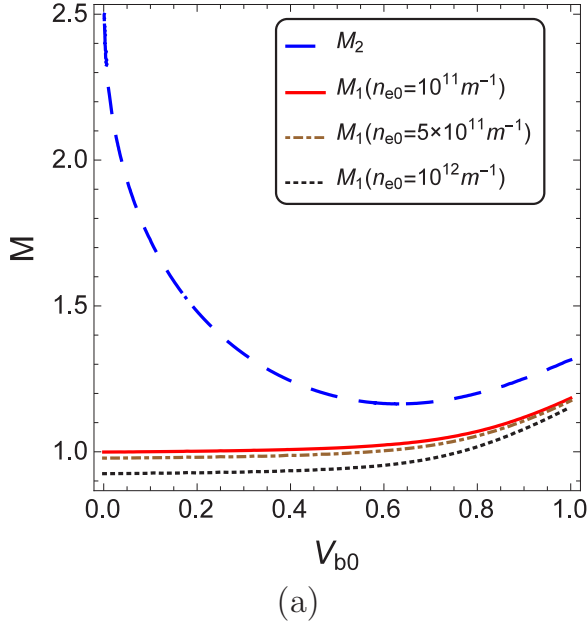

(a)

(b)

FIG. 1. The Mach number M is depicted versus (a) the beam velocity V_{b0} (for $\delta = 0.01$) and (b) the beam density δ (taking $V_{b0} = 0.2$). We have considered different values of the (equilibrium) electron density n_{e0} (as listed in the inset label) and $\mu_b = 1$ (H^+ beam).
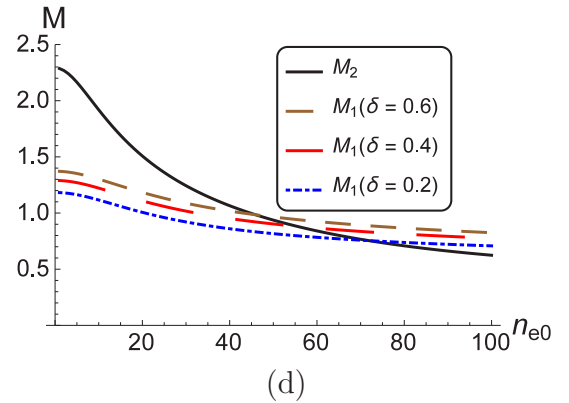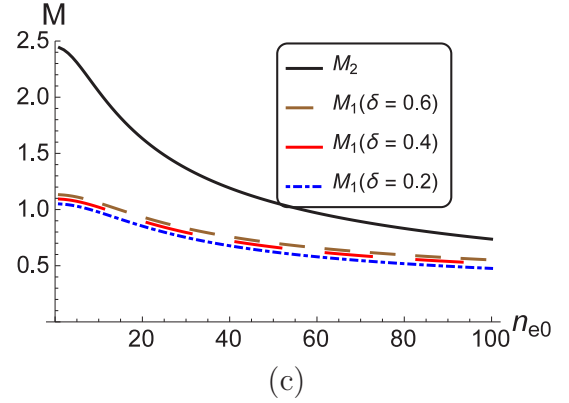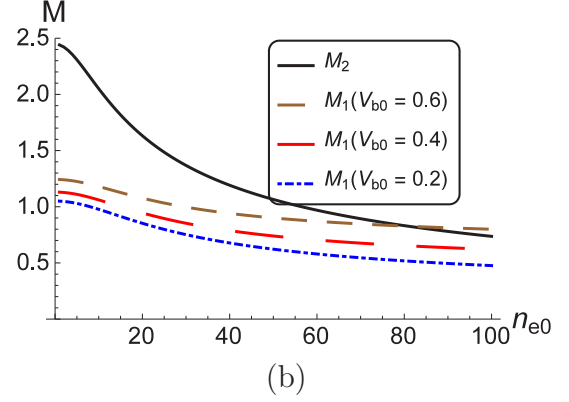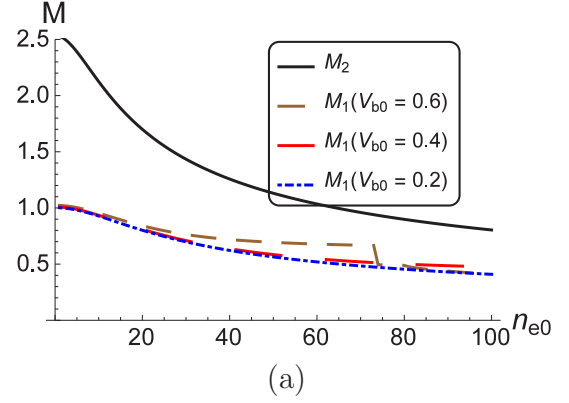

(a)

(b)

(c)

(d)

FIG. 2. The soliton existence region, i.e., the interval of the permitted Mach number M values, is depicted with n_{e0} in units of 10^{11} m^{-1} (a) for different values of V_{b0} with $\delta = 0.01$, (b) for different values of V_{b0} with $\delta = 0.2$, (c) for different values of δ with $V_{b0} = 0.2$, and (d) for different values of δ with $V_{b0} = 0.5$.

nonrelativistic electron Fermi energy $E_{\text{Fe}} = p_{\text{Fe}}^2/2m_e$ (and momentum $p_{\text{Fe}} = hn_{e0}/4$), which in turn prescribes the length scale as c_s/ω_p.

The fluid equations take the following forms:

$$\frac{\partial(\gamma_i n_i)}{\partial t} + \frac{\partial}{\partial x}(\gamma_i n_i u_i) = 0, \tag{10}$$

$$\frac{\partial(\gamma_i u_i)}{\partial t} + u_i \frac{\partial(\gamma_i u_i)}{\partial x} = -\frac{\partial \phi}{\partial x}, \tag{11}$$

$$\frac{\partial(\gamma_e n_e)}{\partial t} + \frac{\partial}{\partial x}(\gamma_e n_e u_e) = 0, \tag{12}$$

$$H\left[\frac{\partial(\gamma_e u_e)}{\partial t} + u_e \frac{\partial(\gamma_e n_e)}{\partial x}\right]$$
$$= \frac{1}{\mu_e}\frac{\partial \phi}{\partial x} - \frac{n_e \gamma_e}{H\mu_e}\left(\frac{\partial n_e}{\partial x} + \alpha u_e \frac{\partial n_e}{\partial t}\right), \tag{13}$$

$$\frac{\partial(\gamma_b n_b)}{\partial t} + \frac{\partial}{\partial x}(\gamma_b n_b u_b) = 0, \tag{14}$$

$$\left[\frac{\partial(\gamma_b u_b)}{\partial t} + u_b \frac{\partial(\gamma_b u_b)}{\partial x}\right] = -\frac{1}{\mu_b}\frac{\partial \phi}{\partial x}, \tag{15}$$

$$\frac{\partial^2 \phi}{\partial x^2} = \gamma_e n_e - \beta \gamma_i n_i - \delta \gamma_b n_b, \tag{16}$$

where $H = \sqrt{1 + \xi^2}$ represents the enthalpy of the system [45], where $\xi = \frac{hn_e}{4m_e c}$; the relativistic factor is redefined as $\gamma_j = 1/\sqrt{1 - \alpha u_j^2}$, where $\alpha = \frac{c_s^2}{c^2} = \mu_e \xi_0^2$. We have also introduced the ion-to-electron charge ratio $\beta = \frac{Z_i n_{i0}}{n_{e0}}$, the beam-to-electron charge density ratio $\delta = \frac{Z_b n_{b0}}{n_{e0}}$, the electron-to-ion mass ratio $\mu_e = \frac{m_e}{m_i}$ ($\simeq 1/1836 \approx 0.0005 \ll 1$), and the mass ratio $\mu_b = \frac{m_b}{m_i}$. Note that overall charge neutrality is assumed at equilibrium (imposing $\beta = 1 - \gamma_{b0}\delta$).

Small-amplitude (harmonic wave) solutions are straightforward to obtain upon linearizing the model equations, Eqs. (10)–(16), above. The linear aspects of the beam-plasma system dynamics resulting from this framework have been analyzed in detail in Ref. [48] and need not be repeated here. Actually, two low-frequency acoustic modes exist, propagating at different phase speeds (associated with the two ionic components), in addition to an electron plasma (Langmuir-type) high-frequency mode [46], whose characteristics reflect the relativistic invariance of the model and also incorporate quantum degeneracy effects (which become important at high densities), just as intuitively anticipated. In the presence of the ion beam [48], the surplus energy destabilizes both low-frequency modes [48], though the associated growth rate is weak for a tenuous beam and operates in a narrow wave-number window.

As a representative "textbook" situation, we henceforth consider a hydrogen plasma ($Z_1 = 1$) and a tenuous beam, i.e., implicitly assuming $\delta \ll 1$ and $\mu_b \sim 1$ throughout.

III. NONLINEAR ANALYSIS

Let us consider a localized perturbation, in the form of a solitary wave propagating with (dimensionless) speed $M = U_{\text{sol}}/c_s$, where c_s here denotes the pseudosound speed, which was defined in the previous section as $c_s = \sqrt{2Z_i E_{\text{Fe}}/m_i}$.

We have adopted here an analogy with the so-called *"Mach number"* in electrostatic soliton theory in classical plasmas [50], a terminology which in turn reflects an analogy with real sound (acoustic) waves propagating in air. We pass from the laboratory frame to the moving reference frame by assuming that all quantities are functions of a single variable $X = x - Mt$, viz.,

$$\frac{\partial}{\partial t} = -M\frac{\partial}{\partial X}, \qquad \frac{\partial}{\partial x} = \frac{\partial}{\partial X}. \tag{17}$$

Combining with the system of Eqs. (10)–(16), we obtain the following system of ordinary differential equations (ODEs):

$$-M(\gamma_i n_i)' + (\gamma_i n_i u_i)' = 0,$$
$$-M(\gamma_e n_e)' + (\gamma_e n_e u_e)' = 0,$$
$$-M(\gamma_b n_b)' + (\gamma_b n_b u_b)' = 0,$$
$$-M(\gamma_i n_i)' + u_i(\gamma_i u_i)' + \phi' = 0,$$
$$-H(M - u_e)(\gamma_e u_e)' + \frac{\gamma_e n_e}{H\mu_e}(1 - \alpha M u_e)u_e' - \frac{1}{\mu_e}\phi' = 0,$$
$$-M(\gamma_b n_b)' + u_b(\gamma_b u_b)' + \frac{1}{\mu_b}\phi' = 0,$$
$$\phi'' = \gamma_e n_e - \beta \gamma_i n_i - \delta \gamma_b n_b. \tag{18}$$

Assuming vanishing boundary conditions for all of the state variables (except the ion beam, which satisfies $\lim_{X \to \pm\infty} u_b =$

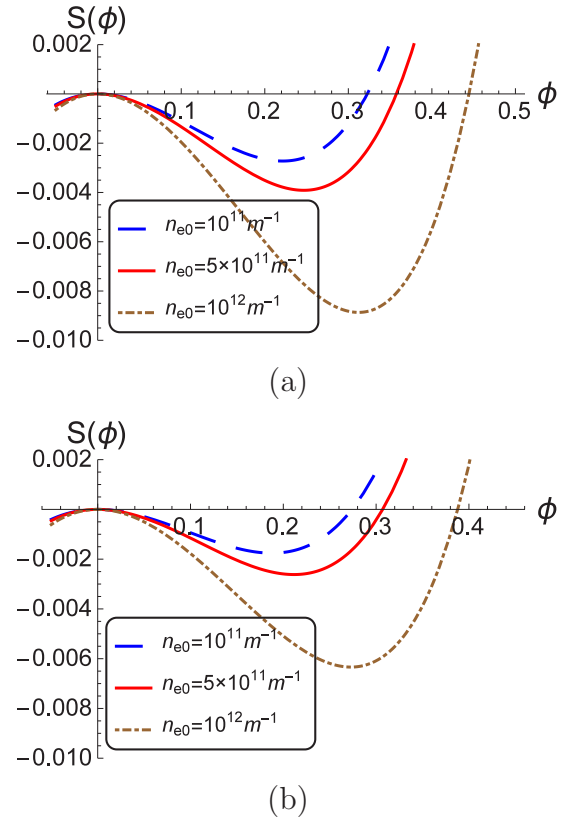FIG. 3. The pseudopotential $S(\phi)$ is depicted in terms of the electrostatic potential ϕ for different values of the unperturbed electron density n_{e0} in two cases: (a) $V_{b0} = 0$ and (b) $V_{b0} = 0.2$. We have assumed $\delta = 0.01$, $\mu_b = 1$, and $M = 1.2$ everywhere.
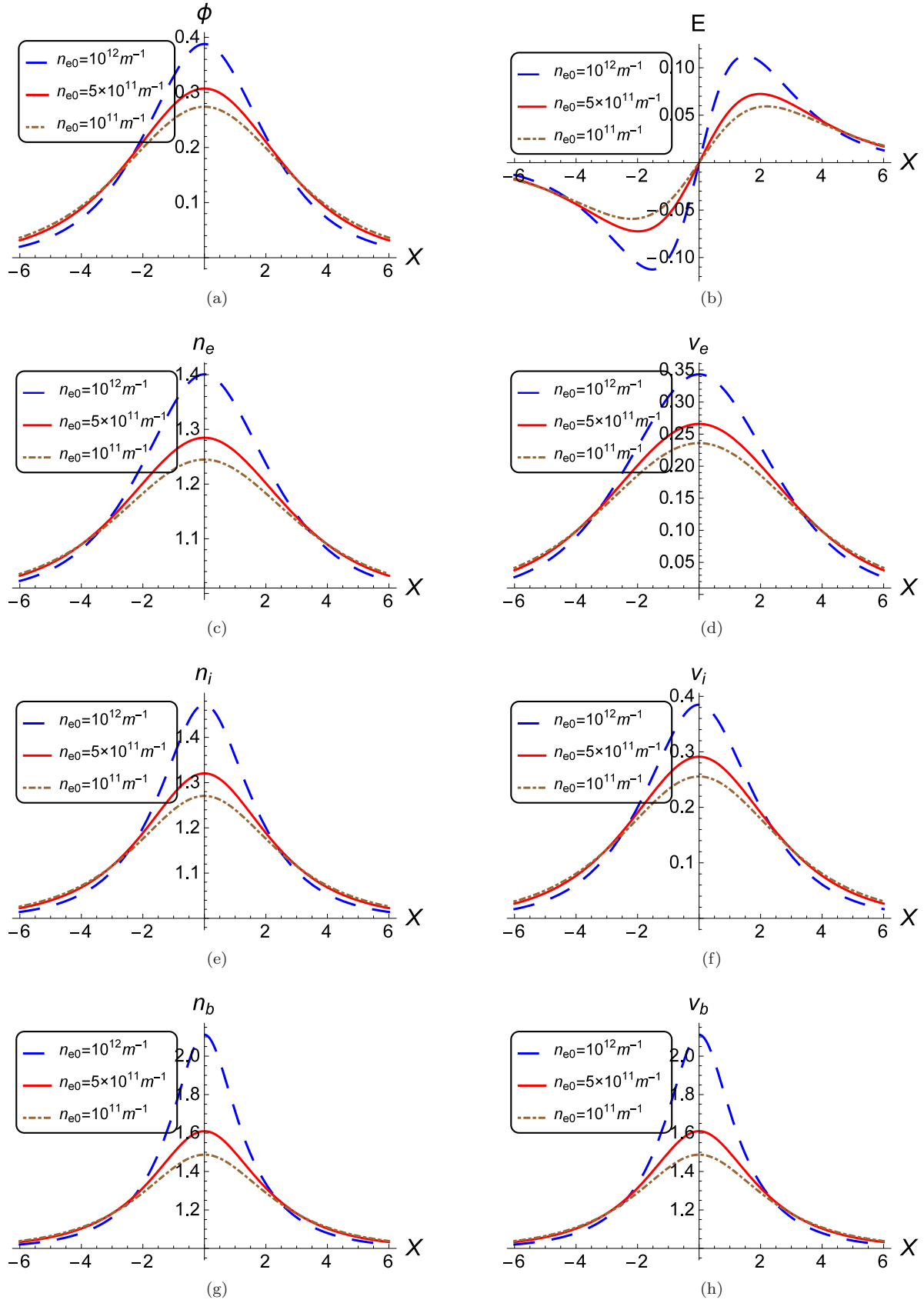
FIG. 4. The plasma (fluid) state variables are shown in terms of the space variable X, for different values of the unperturbed (equilibrium) electron density n_{e0}. We have taken $M = 1.2$, $V_{b0} = 0.2$, $\delta = 0.01$, and $\mu_b = 1$.

V_{b0}), we have manipulated the latter equations into a set of analytical expressions for the ion, beam-ion, and electron fluid density and speed variables, as functions of the electrostatic potential. This was a delicate task, due to the complex structure of the above equations (in comparison, e.g., with classical models [49,50]). The procedure is described in full detail in the Appendix, for reference, yet unnecessary details are omitted below.

After some tedious but straightforward algebra, we obtain an ODE in the form

$$\frac{1}{2}\left(\frac{d\phi}{dX}\right)^2 + S(\phi) = 0. \tag{19}$$

Here, S is a nonlinear function given by

$$S(\phi) = (1 - \gamma_{b0}\delta)S_i(\phi) + \delta[S_{b1}(\phi) - S_{b0}] - [S_{e1}(\phi) - S_{e0}], \tag{20}$$

where

$$S_i(\phi) = Mu_i\gamma_i,$$
$$S_{b1}(\phi) = \mu_b\gamma_{b0}u_b\gamma_b(M - V_{b0}),$$
$$S_{e1}(\phi) = \left[\gamma_e n_e\left(\phi + \frac{H_0}{\xi_0^2}\right)\right.$$
$$\left. - \frac{1}{2\xi_0^3}(\sinh^{-1}(\xi_0 n_e) + \xi_0 n_e H)\right],$$
$$S_{b0} = \mu_b\gamma_{b0}^2 V_{b0}(M - V_{b0}),$$
$$S_{e0} = \frac{H_0}{\xi_0^2} - \frac{1}{2\xi_0^3}(\sinh^{-1}(\xi_0) + \xi_0 H_0). \tag{21}$$

It is easy to identify the contributions of the three plasma components to the latter expression. Note that $S_{j1}(\phi = 0) = S_{j0}$ (for $j = i, e, b$), at equilibrium, while $S_{i1}(\phi = 0) = 0$.

Equation (19) has the form of a pseudo-energy-conservation equation, for a particle of unit mass, where the first term represents a kinetic energy term and $S(\phi)$ is a pseudopotential energy function (assuming that the variable X plays the role of "time" and the potential ϕ plays the role of a virtual "position coordinate" in analogy). This formalism is reminiscent of the Sagdeev-type methodology [49] for localized electrostatic excitations (collisionless shocks) in plasmas [50]; details can be found in related literature (see, e.g., in Ref. [50] for a thorough discussion) and are thus omitted here.

The analysis therefore consists of solving Eq. (19) (numerically) for the electrostatic potential $\phi(X)$ and then calculating the remaining plasma variables (as functions of space), in the moving frame. Examples of the outcome of this procedure are presented in the parametric analysis that follows.

IV. EXISTENCE CONDITIONS FOR SOLITARY WAVES

It is anticipated, from previous applications of the above methodology in classical plasmas [45,50], that the soliton speed M must take values included in an interval (M_1, M_2) for solutions to exist. The boundaries (M_1, M_2) depend on the particular aspects of the problem, here the plasma configuration and the beam characteristics.

We determine in the following the Mach number limitations and then investigate the effect of the beam on the parameter regions where electrostatic waves may occur. Naturally, in every step in the analysis that follows, the (beam-free) limit $\delta = 0$ recovers the expressions and numerical values found in Ref. [45] for electron-ion plasma.

The pseudopotential S must satisfy a number of conditions in order for solutions to exist. First of all, one may easily check that $S(\phi = 0) = \frac{dS(\phi)}{d\phi}|_{\phi=0} = 0$, reflecting the physical fact that both the electric field and the charge density are zero at equilibrium. Furthermore, the curve must have a maximum at the origin, implying $\frac{d^2S(\phi)}{d^2\phi}|_{\phi=0} < 0$, hence the origin is an unstable fixed point. Finally, we are interested in parameter values for which $S(\phi) < 0$—as is obvious from Eq. (19)—which is realised in the interval $0 < \phi < \phi_0$; here, ϕ_0, say, denotes the first nonzero root of S, viz., $S(\phi_0) = 0$, which represents the maximum value of ϕ to be "visited" by the dynamics.
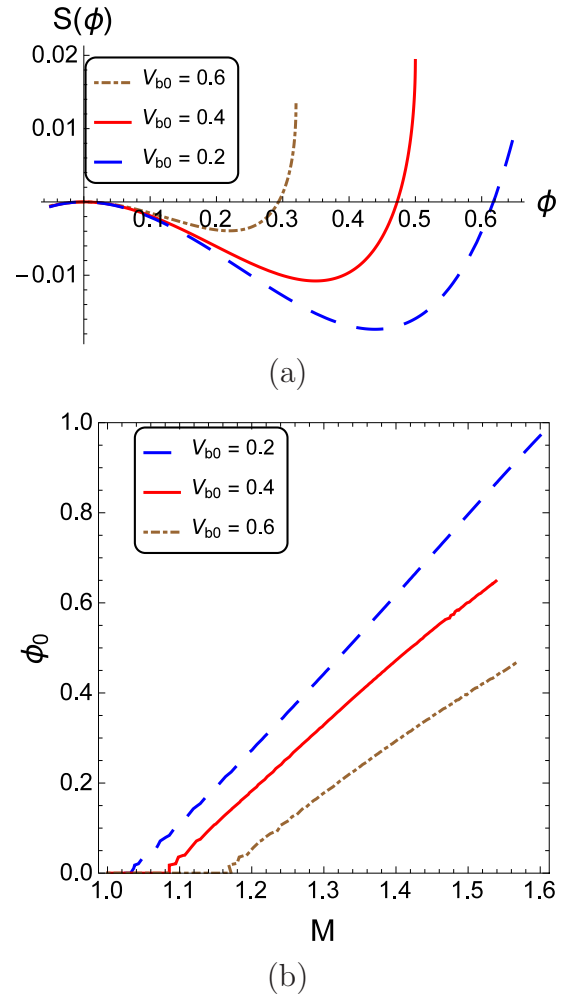

(a)

(b)

FIG. 5. (a) The pseudopotential function $S(\phi)$ is shown in terms of the electrostatic potential ϕ, for different values of the beam velocity V_{b0}. (b) The maximum pulse amplitude ϕ_m is depicted versus the Mach number M, for different values of the (equilibrium) beam velocity V_{b0}. We have taken $n_{e0} = 10^{11}m^{-1}$ (or $\xi_0 = 0.0603798$), $\mu_b = 1$, $\delta = 0.01$, and $M = 1.4$ as indicative values.
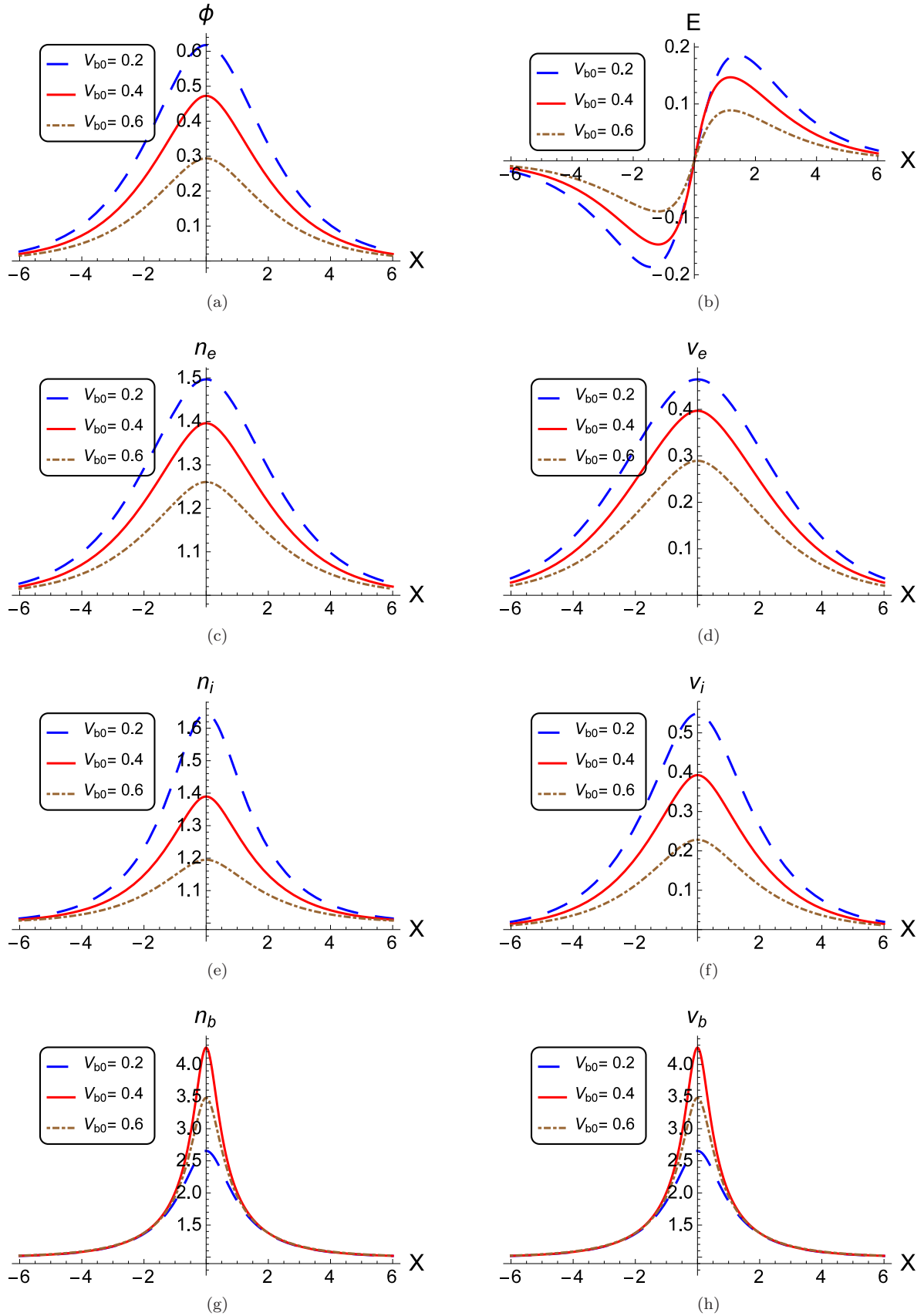
FIG. 6. The plasma state variables are shown in terms of the space variable X, for different values of the ion beam velocity V_{b0}, taking $n_0 = 10^{11} \text{m}^{-1}$ (or $\xi_0 = 0.0603798$), $M = 1.4$, $\delta = 0.01$, and $\mu_b = 1$.

a. Minimum Mach number. The superacoustic condition.
The curvature condition $\frac{d^2 S(\phi)}{d\phi^2} \leqslant 0$ (see above) leads to the inequality

$$
(1 - \gamma_{b0}\delta)\frac{1}{M_1^2} - \frac{H_0}{1 - \mu_e H_0^2 M_1^2}
$$

$$
+ \frac{\delta}{\mu_b}\frac{1 - \alpha V_{b0}\gamma_{b0}^2(M_1 - V_{b0})}{\gamma_{b0}^3(M_1 - V_{b0})^2} \leqslant 0. \tag{22}
$$

The lower boundary for the Mach number, say M_1, is thus obtained by solving the equation $S''(\phi = 0; M_1) = 0$ for M_1.

b. Maximum Mach number. A second physical requirement is associated with the reality of the state variables, i.e., the density variables n_j and the fluid speed variables (for $j = e,i,b$). First of all, from the analytical expression for the ion fluid speed—see Eq. (A6) in the Appendix—we obtain an explicit requirement for u_i to be real, in the form of the following inequality:

$$
\phi \leqslant \phi_{\max,i} = \frac{1}{\alpha}(1 - \sqrt{1 - \alpha M^2}). \tag{23}
$$

In the nonrelativistic limit $\alpha \ll 1$, this condition reduces to $\phi \leqslant \phi_{\max,i} = \frac{M^2}{2}$, which is the well-known classical requirement [49].

Following a similar argument, from Eq. (A10) (in the Appendix) for the beam fluid speed, we find the following condition to be imposed, for reality:

$$
\phi \leqslant \phi_{\max,b} = \frac{\mu_b}{\alpha}[\gamma_{b0}(1 - MV_{b0}\alpha) - \sqrt{1 - M^2\alpha}], \tag{24}
$$

In the nonrelativistic limit $\alpha \ll 1$, we obtain $\phi_{\max,b} = \frac{\mu_b}{2}(M - V_{b0})^2$; hence for $V_{b0} = 0$, we recover $\phi_{\max,b} = \frac{M^2}{2}$, in agreement with the infinite compression limit in the classical case [49,50]. We see that a maximum value must be imposed for the electrostatic potential ϕ, viz., $\phi \leqslant \min\{\phi_{\max,i}, \phi_{\max,b}\} \equiv \phi_m$. In the above considerations, it is understood that $M < 1/\sqrt{\alpha}$, a condition which indeed holds for all realistic parameter values to be adopted in the following.

In view of the above reality requirement(s), we impose the condition

$$
S(\phi_m) \geqslant 0, \tag{25}
$$

where ϕ_m was defined above. The upper boundary M_2 is thus obtained by solving the equation $S(\phi = \phi_m; M_2) = 0$ (numerically) for M_2.

In order to determine the soliton existence region, and to elucidate the role of the beam (characteristics), we have numerically solved Eqs. (22) and (25) for the limit values M_1 and M_2, respectively, assuming a positive hydrogen beam ($\mu_b = 1$), for various combinations of values for the beam speed (V_{b0}), the density (δ), and the unperturbed electron density n_{e0}.

Figure 1(a) shows the variation of M_1 with the ion beam velocity V_{b0}, for certain (fixed) values of n_{e0}, μ_b, and δ. We can see that M_1 increases with the beam velocity V_{b0}. In an analogous manner, Fig. 1 shows that M_1 is an increasing function of the beam density δ (for given values of n_{e0}, μ_b, and V_{b0}). In both cases, however, M_1 decreases upon increasing the density n_{e0}.

The permitted range of values for $M \in [M_1, M_2]$ was found numerically and is depicted in Fig. 2, against the electron density n_{e0} (for given fixed values of V_{b0} δ). Solutions occur between the lower and upper curves in this plot. We note that the upper curve decreases faster, for higher values of the electron density n_{e0}, until it crosses over. Solutions will not exist beyond this crossover point.

V. PARAMETRIC ANALYSIS

We have solved Eqs. (19) and (20) numerically for various values of the plasma configuration parameters (n_{e0}, V_{b0}, δ, and M), keeping the value of μ_b fixed (to one). The results are shown in Figs. 3–8. We have studied the effect of the physical plasma parameters on the shape of the Sagdeev potential, the maximum amplitude of electrostatic potential ϕ_m, the corresponding electric field E, and plasma state variables n_e, u_e, n_i, u_i, n_b, and u_b; these are discussed in the following.
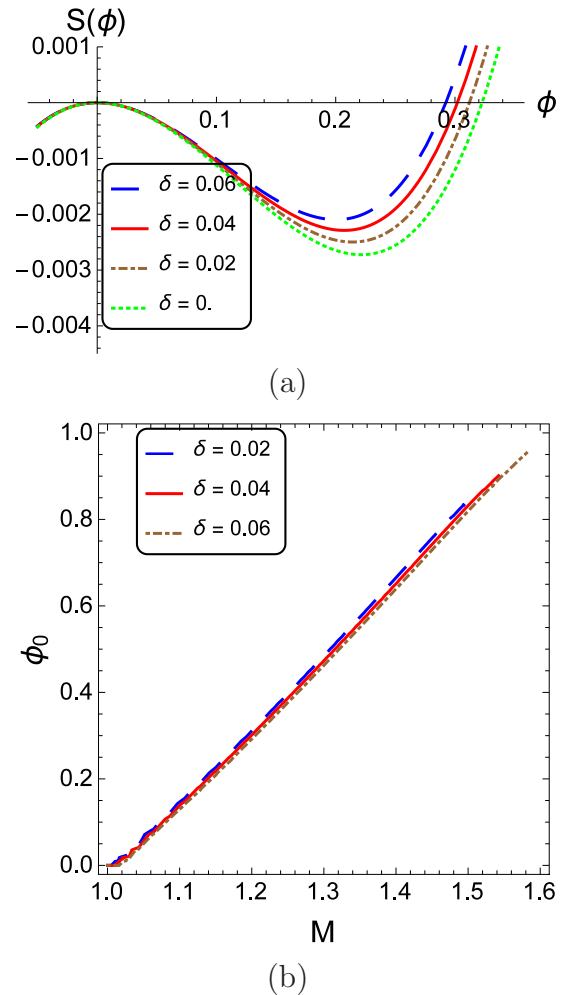

(a)

(b)

FIG. 7. (a) The pseudopotential $S(\phi)$ is shown in terms of the electrostatic potential ϕ for different values of the unperturbed beam density δ. (b) The maximum pulse amplitude ϕ_m is shown versus the Mach number M. We have taken $V_{b0} = 0.2$, $n_{e0} = 10^{11}$ m^{-1} (or $\xi_0 = 0.0603798$), $\mu_b = 1$, and $M = 1.2$ as indicative values.
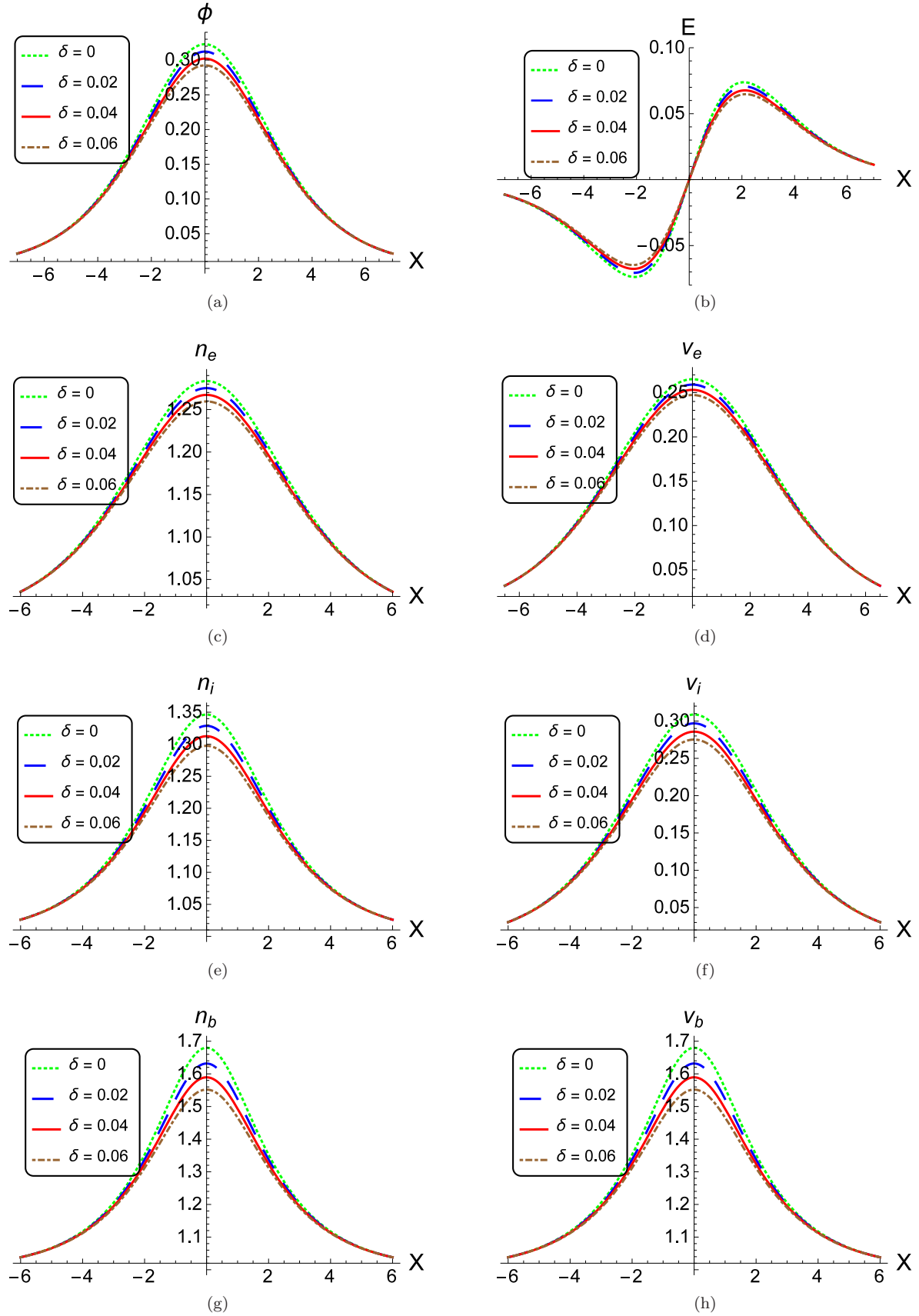
FIG. 8. The plasma state variables are shown in terms of the space variable X, for different values of the beam density δ, with $n_{e0} = 10^{11} m^{-1}$ (or $\xi_0 = 0.0603798$), $M = 1.2$, $V_{b0} = 0.2$, and $\mu_b = 1$.

A. The effect of the equilibrium electron density

To study the effect of the asymptotic (equilibrium) electron density n_{e0}, we have plotted the pseudopotential $S(\phi)$, given by Eq. (20), for different values of n_{e0} in Fig. 3. The corresponding electrostatic potential ϕ and the resulting ambipolar electric field E, in addition to the plasma state variables (namely, the elecron density n_e, the electron velocity u_e, the ion density n_i, the ion velocity u_i, the ion beam density n_b, and the ion beam velocity u_b), were found numerically and are shown in Fig. 4. We see in Fig. 3 that the root of $S(\phi)$ increases monotonically with n_{e0}, suggesting stronger potential pulses at larger densities. Furthermore, the depth of the Sagdeev potential well increases with n_e0. We can see from Fig. 4(a) that the amplitude of the electrostatic potential (pulse) ϕ increases with n_{e0}, while the width decreases; the pulse therefore becomes narrower (steeper) for higher n_{e0}. An analogous variation of all other plasma state variables is visible in Figs. 4(b)–4(h).

B. Beam velocity effect

We have plotted the Sagdeev pseudopotential $S(\phi)$ against ϕ in Fig. 5, for different values of the (equilibrium) beam fluid speed V_{b0}. Both the root of S (i.e., the maximum value of the potential ϕ excitation) and the depth of the potential well are seen to *decrease* with larger V_{b0}. The corresponding plasma state variables were obtained numerically and are shown in Fig. 6. We see that the amplitude (width) of all plasma variables increases (decreases) with larger beam velocity value.

C. The effect of the equilibrium beam density

Finally, we have varied the value of the ion beam density δ in order to study its effect on the shape of the Sagdeev potential in Fig. 7. Furthermore, its effect (for fixed speed V_{b0}) on the amplitude and the width of the associated electrostatic pulse and electric field is shown in Fig. 8. The conclusions to be drawn from this analysis are directly analogous to the ones deduced from varying the beam velocity in the previous paragraph, as qualitatively expected. Indeed, an increase in either the beam (fluid) speed or the beam density results in an increase in the beam (and, in fact, overall) current J, which therefore affects the propagation characteristics of electrostatic solitary waves. We have kept the value of the beam current very low in our sets of numerical values considered, with respect to the electrostatic approximation (i.e., so as to justify having neglected dynamical magnetic field generation in our model).

VI. CONCLUSIONS

We have established a rigorous relativistic model for electrostatic excitations in ultradense plasma (assuming quantum degeneracy for the electrons), and we have used it as a basis to study the influence of a positive ion beam onto electrostatic solitary waves propagating in the plasma. Nonlinear analysis has revealed that positive potential ϕ (only) pulses may occur, in agreement with experiments on laser-plasma interactions [52,53]. The existence domain (velocity, or Mach number interval) of solitary waves has been determined and shown to become slightly wider with an increase in beam density

while, reversely, it "shrinks" dramatically with an increase in beam velocity (for fixed density). Finally, we have studied the effect of intrinsic plasma parameters on the structural properties (shape) of solitary waves.

Our nonlinear analysis has focused on large electrostatic excitations and thus has imposed no restriction on their amplitude, which was left arbitrary throughout the study. An independent, linear analysis would have led to small-amplitude harmonic solutions, i.e., Fourier modes (electrostatic waves), along the lines proposed, e.g., in Ref. [46] (in the absence of a beam). We point out that the latter study led to a dispersion relation which was characterized by two distinct dispersion branches (for the *real* frequency ω as a function of the wave number k), namely, an acoustic one and an (Langmuir-like) electron-plasma branch. In the presence of an ion beam, however, the dispersion relation becomes a sixth-order polynomial, whose analysis reveals the existence of a third (beam-driven) mode [48]. In addition to this qualitative change, due to the beam, an imaginary part γ arises in the (now complex) frequency, say $\omega = \omega_r + i\gamma$, in a small window of values of the wave number k; hence a linear instability develops [48]. Admittedly, both the beam-ion component number density and the velocity were assumed to be small, with respect to the electrostatic approximation (i.e., in order for the total current to be negligible and hence the magnetic field generation to be suppressed); hence the growth rate of this linear instability should be thought of as small, for practical situations. However, a stronger beam should lead to a growing mode which might be dominant and eventually destabilize the electrostatic wave. From a purely energetic view point, this would represent a loss term, which should eventually destabilize not only linear waves but also localized lumps of energy (solitary waves) occurring in the system.

Apart from the aforementioned (linear) beam instability, one might expect solitary wave propagation to be affected by nonlinear beam plasma or kinetic instabilities, such as Buneman-type instabilities [54,55] or even Landau damping [56,57], a kinetic effect expectedly overlooked in the fluid picture adopted herein.

Our results are expected to be important in dense plasmas arising from solid target irradiation by ultrahigh-intensity laser beams and also in extreme astrophysical environments, where high-density plasma models are relevant.

APPENDIX: DERIVATION OF EXPRESSIONS FOR THE STATE VARIABLES IN THE MOVING FRAME

All of the plasma state variables are assumed to obey constant boundary values at infinity, i.e., $\lim_{X\to\pm\infty} n_{i,e,b} = 1$, $\lim_{X\to\pm\infty} u_{i,e} = 0$, $\lim_{X\to\pm\infty} u_b = V_{b0}$, and $\lim_{X\to\pm\infty} \phi = 0$. One can integrate the continuity equations, the first three equations in Eq. (18), for the ion, the electron, and the beam-ion density, to obtain

$$n_i = \frac{M}{\gamma_i(M - u_i)}, \tag{A1}$$

$$n_e = \frac{M}{\gamma_e(M - u_e)}, \tag{A2}$$

$$n_b = \frac{\gamma_{b0}(M - V_{b0})}{\gamma_b(M - u_b)}, \tag{A3}$$

where $\gamma_{b0} = 1/\sqrt{1 - \alpha V_{b0}^2}$. By integrating the equation of motion (19) for the ions, we obtain

$$\phi = M\gamma_i u_i - \frac{\gamma_i}{\alpha} + \frac{1}{\alpha}, \tag{A4}$$

i.e.,

$$\left[M^2 + \alpha\left(\frac{1}{\alpha} - \phi\right)^2\right]u_i^2 - \frac{2M}{\alpha}u_i + \left[\frac{1}{\alpha^2} - \left(\frac{1}{\alpha} - \phi\right)^2\right] = 0. \tag{A5}$$

The solution for the ion fluid speed reads

$$u_i = \frac{\frac{M}{\alpha} - \sqrt{\frac{M^2}{\alpha^2} - \left[M^2 + \alpha\left(\frac{1}{\alpha} - \phi\right)^2\right]\left[\frac{1}{\alpha^2} - \left(\frac{1}{\alpha} - \phi\right)^2\right]}}{M^2 + \alpha\left(\frac{1}{\alpha} - \phi\right)^2}, \tag{A6}$$

where we chose to proceed with the solution satisfying the boundary condition $\lim_{X\to\pm\infty} \phi = \lim_{X\to\pm\infty} u_i = 0$. A thorough analysis of the quantity under the square root reveals that reality of the ion fluid speed (A6) imposes

$$\phi \leqslant \frac{1}{\alpha}(1 - \sqrt{1 - \alpha M^2}). \tag{A7}$$

In an analogous manner, upon integrating the equation of motion (19) for the beam (fluid), we obtain

$$\frac{1}{\mu_b}\phi = M(\gamma_b u_b - \gamma_{b0} V_{b0}) - \frac{\gamma_b}{\alpha} + \frac{\gamma_{b0}}{\alpha} \tag{A8}$$

or, rearranging,

$$\left\{M^2 + \alpha\left[\gamma_{b0}\left(M V_{b0} - \frac{1}{\alpha}\right) + \frac{1}{\mu_b}\phi\right]^2\right\}u_b^2 - \frac{2M}{\alpha}u_b + \left\{\frac{1}{\alpha^2} - \left[\gamma_{b0}\left(M V_{b0} - \frac{1}{\alpha}\right) + \frac{1}{\mu_b}\phi\right]^2\right\} = 0. \tag{A9}$$

The solution

$$u_b = \frac{\frac{M}{\alpha} - \sqrt{\frac{M^2}{\alpha^2} - \left\{M^2 + \alpha\left[\gamma_{b0}\left(M V_{b0} - \frac{1}{\alpha}\right) + \frac{1}{\mu_b}\phi\right]^2\right\}\left\{\frac{1}{\alpha^2} - \left[\gamma_{b0}\left(M V_{b0} - \frac{1}{\alpha}\right) + \frac{1}{\mu_b}\phi\right]^2\right\}}}{M^2 + \alpha\left[\gamma_{b0}\left(M V_{b0} - \frac{1}{\alpha}\right) + \frac{1}{\mu_b}\phi\right]^2} \tag{A10}$$

satisfies the boundary conditions $\lim_{X\to\pm\infty} \phi = 0$ and $\lim_{X\to\pm\infty} u_b = V_{b0}$. In order for the beam velocity u_b to be a real quantity, the condition

$$\phi \leqslant \frac{\mu_b}{\alpha}[\gamma_{b0}(1 - M V_{b0}\alpha) - \sqrt{1 - M^2\alpha}] \tag{A11}$$

must hold.

Combining Eqs. (A1) and (A6), we obtain the ion fluid density $n_i(\phi)$ and speed $u_i(\phi)$ in terms of the potential ϕ (for a given value of M). The beam-ion fluid properties are obtained in an analogous manner from Eqs. (A3) and (A10).

Integrating the equation of motion of the electrons (19), we obtain

$$\frac{\mu_e}{\alpha}\phi = \left[\gamma_e\sqrt{1 + \frac{\alpha}{\mu_e}n_e^2}(1 - \alpha M u_e) - H_0\right] \tag{A12}$$

or, after some tedious algebra,

$$\left[\xi_0^2(1 - \alpha M^2)\right]n_e^4 + \left[1 - \left(\xi_0^2\phi + H_0\right)^2 - \alpha M^2\left(1 - \xi_0^2\right)\right]n_e^2 + \alpha M^2 = 0. \tag{A13}$$

The electron density is thus given, in terms of ϕ, by the biquadratic polynomial equation

$$n_e(\phi) = \sqrt{\frac{-\left[1 - \left(\xi_0^2\phi + H_0\right)^2 - \alpha M^2\left(1 - \xi_0^2\right)\right] + \sqrt{\left[1 - \left(\xi_0^2\phi + H_0\right)^2 - \alpha M^2\left(1 - \xi_0^2\right)\right]^2 - 4\xi_0^2(1 - \alpha M^2)\alpha M^2}}{2\xi_0^2(1 - \alpha M^2)}}. \tag{A14}$$

Finally, in order to obtain the electron fluid speed in terms of ϕ, we substitute Eq. (A14) into Eq. (A2).

Combining the above relations for the density variables into Poisson's equation (19), we find, for the electrostatic potential ϕ, a differential equation in the form

$$\frac{d^2\phi}{dX^2} = f(\phi), \tag{A15}$$

where the function f in the RHS is given by

$$f(\phi) = -\frac{\alpha M^2}{1 - \alpha M^2}$$

$$+ \frac{\sqrt{\alpha M^2 + \frac{\mu_e}{2\alpha}\left\{\sqrt{\left[1 - \left(\xi_0^2\phi + H_0\right)^2 - \alpha M^2\left(1 - \xi_0^2\right)\right]^2 - 4\xi_0^2(1 - \alpha M^2)\alpha M^2} - \left[1 - \left(\xi_0^2\phi + H_0\right)^2 - \alpha M^2\left(1 - \xi_0^2\right)\right]\right\}}}{1 - \alpha M^2}$$

$$- (1 - \gamma_{b0}\delta)\frac{M}{M - \frac{\frac{M}{\alpha} - \sqrt{\frac{M^2}{\alpha^2} - \left[M^2 + \alpha\left(\frac{1}{\alpha} - \phi\right)^2\right]\left[\frac{1}{\alpha^2} - \left(\frac{1}{\alpha} - \phi\right)^2\right]}}{M^2 + \alpha\left(\frac{1}{\alpha} - \phi\right)^2}}$$

$$- \delta\frac{\gamma_{b0}(M - V_{b0})}{M - \frac{\frac{M}{\alpha} - \sqrt{\frac{M^2}{\alpha^2} - \left\{M^2 + \alpha\left[\gamma_{b0}\left(MV_{b0} - \frac{1}{\alpha}\right) + \frac{1}{\mu_b}\phi\right]^2\right\}\left\{\frac{1}{\alpha^2} - \left[\gamma_{b0}\left(MV_{b0} - \frac{1}{\alpha}\right) + \frac{1}{\mu_b}\phi\right]^2\right\}}}{M^2 + \alpha\left[\gamma_{b0}\left(MV_{b0} - \frac{1}{\alpha}\right) + \frac{1}{\mu_b}\phi\right]^2}}. \tag{A16}$$

Multiplying by the derivative $d\phi/dX$ and integrating, we obtain precisely Eq. (19):

$$\frac{1}{2}\left(\frac{d\phi}{dX}\right)^2 + S(\phi) = 0, \tag{A17}$$

where S is the nonlinear function given by Eq. (A17) in the text.

---

[1] D. A. Uzdensky and S. Rightley, Rep. Prog. Phys. **77**, 036902 (2014).

[2] V. E. Fortov, Phys. Usp. **52**, 615 (2009).

[3] G. Manfredi and P. A. Hervieux, Appl. Phys. Lett. **91**, 061108 (2007).

[4] H. A. Atwater, Sci. Am. **296**, 56 (2007).

[5] S. A. Wolf *et al.*, Science **294**, 1488 (2001).

[6] M. P. Robinson, B. Laburthe Tolra, M. W. Noel, T. F. Gallagher, and P. Pillet, Phys. Rev. Lett. **85**, 4466 (2000).

[7] G. Manfredi and J. Hurst, Plasma Phys. Controlled Fusion **57**, 054004 (2015).

[8] Yu. Tyshetskiy, S. V. Vladimirov, and R. Kompaneets, Phys. Plasmas **18**, 112104 (2011).

[9] D. Melrose, *Quantum Plasmadynamics: Unmagnetized Plasmas* (Springer, New York, 2008).

[10] F. Haas, *Quantum Plasmas: An Hydrodynamic Approach* (Springer, New York, 2011).

[11] P. K. Shukla and B. Eliasson, Phys. Usp. **53**, 51 (2010).

[12] P. K. Shukla and B. Eliasson, Rev. Mod. Phys. **83**, 885 (2011).

[13] G. Brodin, M. Marklund, J. Zamanian, and M. Stefan, Plasma Phys. Controlled Fusion **53**, 074013 (2011).

[14] C. M. Celata, F. M. Bieniosek, E. Henestroza, J. W. Kwan, E. P. Lee, G. Logan, L. Prost, P. A. Seidl, J.-L. Vay, W. L. Waldron *et al.*, Phys. Plasmas **10**, 2064 (2003).

[15] W. M. Sharp *et al.*, Fusion Sci. Technol. **43**, 393 (2003).

[16] R. C. Davidson, B. G. Logan, J. J. Barnard *et al.*, J. Phys. IV France **133**, 731 (2006).

[17] K. Krushelnick *et al.*, IEEE Trans. Plasma Sci. **28**, 1110 (2000).

[18] I. D. Kaganovich, E. A. Startsev, A. B. Sefkow, and R. C. Davidson, Phys. Rev. Lett. **99**, 235002 (2007).

[19] T. J. Renk, G. A. Mann, and G. A. Torres, Laser Part. Beams **26**, 545 (2008).

[20] S. Ter-Avetisyan, M. Schnürer, R. Polster, P. V. Nickles, and W. Sandner, Laser Part. Beams **26**, 637 (2008).

[21] S. Colak, B. J. Fitzpatrick, and R. N. Bhargava, J. Cryst. Growth **72**, 504 (1985).

[22] A. L. Gurskii, E. V. Lutsenko, A. I. Mitcovets, and G. P. Yablonskii, Phys. B **185**, 505 (1993).

[23] M. E. Yahia, I. M. Azzouz, and W. M. Moslem, Appl. Phys. Lett. **103**, 082105 (2013).

[24] A. H. Sorensen and E. Bonderup, Nucl. Instrum. Methods Phys. Res. **215**, 27 (1983).

[25] S. R. Goldman and I. Hofmann, IEEE Trans. Plasma Sci. **18**, 789 (1990).

[26] E. Witt and W. Lotko, Phys. Fluids **26**, 2176 (1983).

[27] I. D. Kaganovich, E. A. Startsev, and R. C. Davidson, Phys. Plasmas **11**, 3546 (2004).

[28] N. S. Saini and I. Kourakis, Plasma Phys. Controlled Fusion **52**, 075009 (2010).

[29] Q. Lu, S. Wang, and X. Dou, Phys. Plasmas **12**, 072903 (2005).

[30] E. J. Koen, A. B. Collier, and S. K. Maharaj, Phys. Plasmas **19**, 042101 (2012).

[31] M. E. Dieckmann, H. Ahmed, G. Sarri, D. Doria, I. Kourakis, L. Romagnani, M. Pohl, and M. Borghesi, Phys. Plasmas **20**, 042111 (2013).

[32] E. J. Koen, A. B. Collier, and S. K. Maharaj, Phys. Plasmas **21**, 092105 (2014).

[33] K. Baumgärtel, Ann. Geophys. **32**, 1025 (2014).

[34] V. I. Berezhiani, N. L. Shatashvili, and N. L. Tsintsadze, Phys. Scr. **90**, 068005 (2015).

[35] M. Dunne, Nat. Phys. **2**, 2 (2006).

[36] D. Seipt, T. Heinzl, M. Marklund, and S. S. Bulanov, Phys. Rev. Lett. **118**, 154803 (2017).

[37] M. Borghesi, S. Bulanov, D. H. Campbell, R. J. Clarke, T. Z. Esirkepov, M. Galimberti, L. A. Gizzi, A. J. Mackinnon, N. M. Naumova, F. Pegoraro, H. Ruhl, A. Schiavi, and O. Willi, Phys. Rev. Lett. **88**, 135002 (2002).

[38] G. Sarri, D. K. Singh, J. R. Davies, F. Fiuza, K. L. Lancaster, E. L. Clark, S. Hassan, J. Jiang, N. Kageiwa, N. Lopes, A. Rehman, C. Russo, R. H. H. Scott, T. Tanimoto, Z. Najmudin, K. A. Tanaka, M. Tatarakis, M. Borghesi, and P. A. Norreys, Phys. Rev. Lett. **105**, 175007 (2010).

[39] L. Romagnani, A. Bigongiari, S. Kar, S. V. Bulanov, C. A. Cecchetti, T. Zh. Esirkepov, M. Galimberti, R. Jung, T. V. Liseykina, A. Macchi, J. Osterholz, F. Pegoraro, O. Willi, and M. Borghesi, Phys. Rev. Lett. **105**, 175002 (2010).

[40] N. M. Naumova, S. V. Bulanov, T. Zh. Esirkepov, D. Farina, K. Nishihara, F. Pegoraro, H. Ruhl, and A. S. Sakharov, Phys. Rev. Lett. **87**, 185004 (2001).

[41] T. Esirkepov, K. Nishihara, S. V. Bulanov, and F. Pegoraro, Phys. Rev. Lett. **89**, 275002 (2002).

[42] D. Farina and S. V. Bulanov, Plasma Phys. Controlled Fusion **47**, A73 (2005).

[43] G. Sánchez-Arriaga, E. Siminos, V. Saxena, and I. Kourakis, Phys. Rev. E **91**, 033102 (2015).

[44] G. Sánchez-Arriaga and E. Siminos, J. Phys. A: Math. Theor. **50**, 185501 (2017).

[45] M. McKerr, F. Haas, and I. Kourakis, Phys. Rev. E **90**, 033112 (2014).

[46] I. Kourakis, M. McKerr, I. S. Elkamash, and F. Haas, Plasma Phys. Controlled Fusion **59**, 105013 (2017).

[47] N. A. Krall and A. W. Trivelpiece, *Principles of Plasma Physics* (McGraw–Hill, New York, 1973); R. A. Cairns, *Plasma Physics* (Blackie & Son, Glasgow, 1985); F. F. Chen, *Introduction to Plasma Physics and Controlled Fusion*, Volume 1: Plasma Physics (Plenum, New York, 1990).

[48] I. S. Elkamash, F. Haas, and I. Kourakis, Phys. Plasmas **24**, 092119 (2017).

[49] R. Z. Sagdeev, Cooperative phenomena and shock waves in collisionless plasmas, in *Reviews of Plasma Physics*, Vol. 4, edited by M. A. Leontovich (Consultants Bureau, New York, 1966), p. 52.

[50] F. Verheest and M. A. Hellberg, Electrostatic solitons and Sagdeev pseudopotentials in space plasmas: Review of recent advances, in *Handbook of Solitons: Research, Technology, and Applications*, edited by S. P. Land and S. H. Bedore (Nova Science, Hauppauge, NY, 2009).

[51] P. H. Chavanis, Phys. Rev. D **76**, 023004 (2007).

[52] L. Romagnani, S. V. Bulanov, M. Borghesi, P. Audebert, J. C. Gauthier, K. Lowenbruck, A. J. Mackinnon, P. Patel, G. Pretzler, T. Toncian, and O. Willi, Phys. Rev. Lett. **101**, 025004 (2008).

[53] H. Ahmed, M. E. Dieckmann, L. Romagnani, D. Doria, G. Sarri, M. Cerchez, E. Ianni, I. Kourakis, A. L. Giesecke, M. Notley, R. Prasad, K. Quinn, O. Willi, and M. Borghesi, Phys. Rev. Lett. **110**, 205001 (2013).

[54] F. Haas, B. Eliasson, and P. K. Shukla, Phys. Rev. E **86**, 036406 (2012).

[55] F. Haas and A. Bret, Europhys. Lett. **97**, 26001 (2012).

[56] J. Daligault, Phys. Plasmas **21**, 040701 (2014).

[57] J. T. Mendonça and A. Serbeto, Phys. Scr. **91**, 095601 (2016).